Available online at www.sciencedirect.com

ScienceDirect

Ceramics International 34 (2008) 1127–1130

CERAMICS
INTERNATIONAL

www.elsevier.com/locate/ceramint

Characterization of SnO_2 nanowires synthesized from SnO by carbothermal reduction process

S. Thanasanvorakun *, P. Mangkorntong, S. Choopun, N. Mangkorntong

Department of Physics, Faculty of Science, Chiang Mai University, Chiang Mai 50200, Thailand

Abstract

In this paper, single-crystalline SnO_2 nanowires have been successfully prepared by a carbothermal reduction process employing SnO as the starting material and CuO as the catalyst. Their morphologies, purity and sizes of the products were characterized by transmission electron microscopy (TEM), selected area electron diffraction, X-ray diffraction, field emission scanning electron microscopy (FESEM) and Raman spectroscopy, respectively. The FESEM images reveal wire-like and rod-shaped nanowires of about 100–800 μm in length and 30–200 nm in the transverse dimensions. The three observed Raman peaks at 474, 634 and 774 cm^{-1} indicate the typical rutile phase of the SnO_2 which is in agreement with the X-ray diffraction results. The influence of some reaction parameters, including the temperature and the reaction duration, on the forming, morphology and particle size of SnO_2 crystallize is discussed.

Keywords: Carbothermal reduction; Nanowires; SnO_2; SnO

1. Introduction

Recently, semiconducting oxide 1D nanomaterials have attracted considerable attention because of their unique electrical [1], optical [2], and mechanical [3] properties as a result of their low dimensionality and the quantum confinement effect [4]. Among these semiconductors, the rutile form of SnO_2 is one of the interesting materials. It is an n-type semiconductor with a wide band gap of 3.6 eV at room temperature, and is well known for its applications in gas sensors [5], capacitors [6], transistors [7], and solar cells [8]. So far, substantial effort has been devoted to the synthesis of various nanostructured SnO_2 materials, such as nanoparticles, nanodiskettes, nanobelts, and nanorods. Thermal evaporation technique seems to be the most popular process, due to its simplicity, low-cost but can generate several types of nanostructures. By this process, SnO_2 nanowires have been successfully synthesized from various starting materials such as oxide (SnO_2 or SnO) powders [9–13]. However, quite high-temperature (1050 °C for SnO and 1350 °C for SnO_2) under inert atmosphere is generally employed.

In this report a new option of SnO_2 nanowire fabrication method has been investigated. Large quantities of SnO_2 nanowires could be synthesized at a lower temperature, of about 800–850 °C from SnO precursor under normal atmospheric pressure with a carbothermal reduction process and employing CuO as a catalyst. The growth mechanisms of these SnO_2 nanostructures and the size effect in optical phonon will be discussed.

2. Experimental procedure

In general, the carbothermal reduction process is a simple process in which powder source materials are vaporized at an elevated temperature and the resultant vapor phase condense under certain conditions (temperature, pressure, atmosphere, etc.) to form the desired products. In this study, the process employing a horizontal tube furnace (100 cm in length), an alumina tube (5 cm in diameter, 120 cm in length) and alumina boat (2 cm in diameter, 3 cm in height) has been carried out for SnO_2 nanowire fabrication. The nanowires were synthesized by using SnO as the starting powder under controlled conditions with CuO catalyst. In this process, SnO (0.3 g, 99%), active carbon (0.4 g) and CuO (1 g, 99%) powders were mixed in a crucible and then placed in an alumina boat. The boat was then

---

* Corresponding author. Tel.: +66 53 943 375; fax: +66 53 357 511.
E-mail address: suvit_th@hotmail.com (S. Thanasanvorakun).

doi:10.1016/j.ceramint.2007.09.092

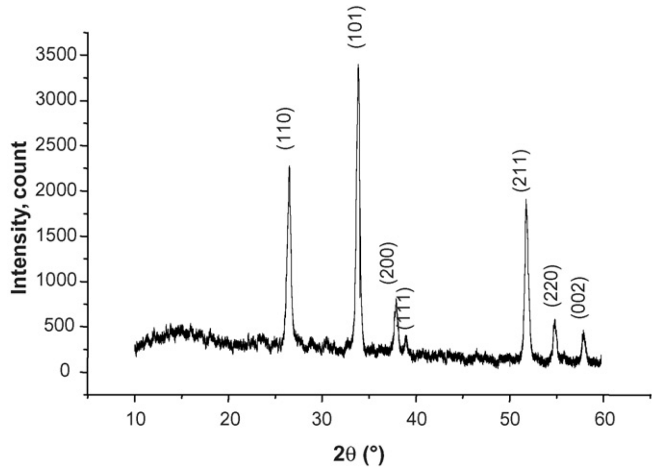

Fig. 1. A typical XRD pattern of the SnO_2 nanowires obtained from Cu Kα radiation.

rapidly heated in a horizontal tube furnace which had been kept at the optimal temperature of 850 °C for 1 h under normal atmospheric pressure. No inert gas was required. After cooling down to room temperature, some white wool-like spots scattered thoroughly in the mixture were observed. The phase of the as-synthesized products were identified by X-ray diffraction (XRD) with Cu Kα radiation ($\lambda = 0.1542$ nm) from 10° to 60° (2θ) in a step of 0.16°. The morphologies and sizes of the products were characterized by scanning electron microscopy (SEM), FEI Quanta 3D (2 0 0) operated at 30 kV. To obtain more information, transmission electron microscopy (TEM) and the typical selected area electron diffraction (SAED) pattern have been taken on JEOL JEM-2010 operated at 200 kV. Raman spectral measurements were performed with JY T64000 under backscatter geometry at room temperature. A green line (514.5 nm) of Ar laser was used as the excitation source with output power of 15 mW.

3. Results and discussion

The X-ray diffraction (XRD) pattern (Fig. 1) of SnO_2 nanowires revealed that there were eight peaks with 2θ values of 26.48°, 33.87°, 37.91°, 38.98°, 51.72°, 54.85°, and 57.97°, corresponding to SnO_2 crystal planes of (1 1 0), (1 0 1), (2 0 0), (1 1 1), (2 1 1), (2 2 0), and (0 0 2), respectively. All the diffraction peaks can be indexed to the tetragonal rutile structure of SnO_2 with lattice constants $a = b = 4.734$ Å and $c = 3.185$ Å, respectively, which are consistent with the standard values of bulk SnO_2 (JCPDS 880287). In addition, no characteristic peaks of CuO, which used in the fabrication method, were observed. Thus, the XRD result implies that the as-synthesized products were pure rutile SnO_2.

Fig. 2 shows the typical scanning electron microscopy (SEM) images of the samples. It revealed that their geometrical structures were wire- and rod-like. Their transverse dimensions were 10–120 nm with the typical size of about 50 nm and their length might be up to several hundreds of micrometers. A bending nanowire, as shown in Fig. 2c, performed high flexibility of these nanowires. In addition to wire-shape, belts-likes were also observed. Typical widths and thickness of the belts-likes were in the range of 30–200 and 10–30 nm, respectively.

To provide further insight into the detailed structure of the SnO_2 nanowires, some images of these wires were taken by TEM and selected area electron diffraction (SAED). Fig. 3a shows a TEM bright field image of a selected nanowire which

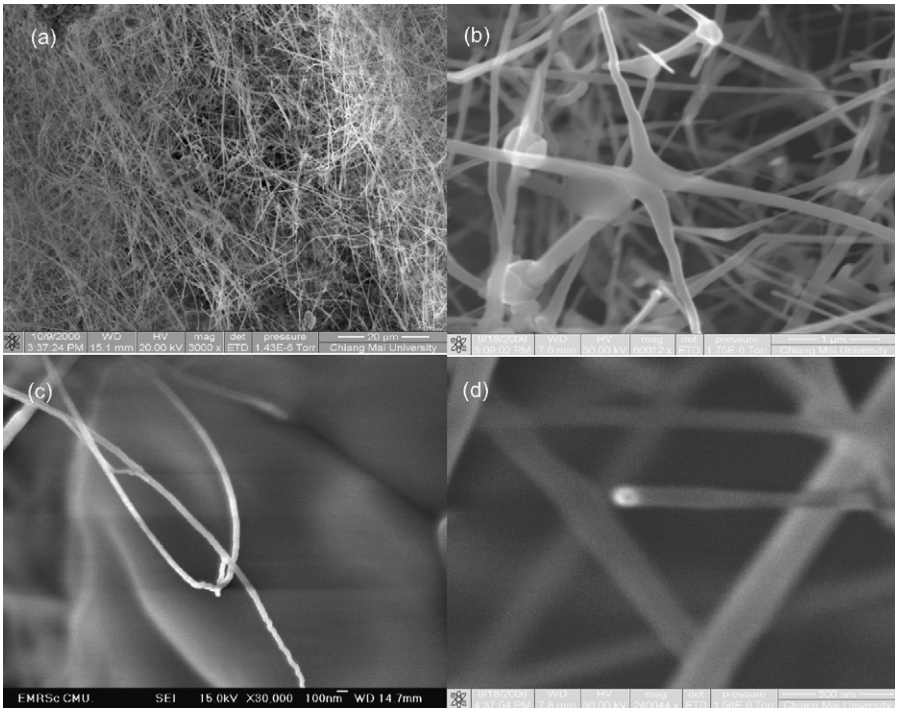

Fig. 2. SEM images of SnO_2 nanowires: (a) a group of nanowires, (b) nanowires combined like star, (c) bending nanowire and (d) nanowire with a tip growth.

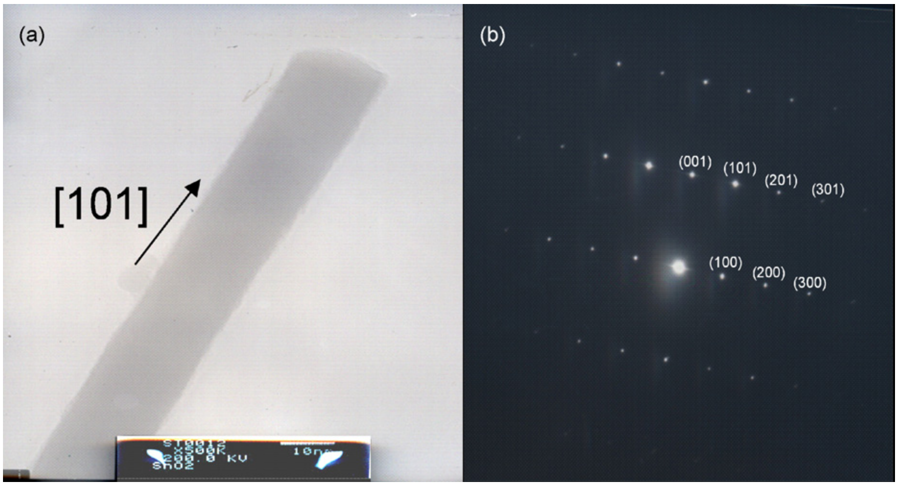

Fig. 3. (a) TEM image of an individual nanowire. (b) SAED pattern taken along [0 2 0].

revealed that it was a single-crystalline without any dislocation. The inset SAED pattern of the nanowires in Fig. 3b was recorded with the electron beam along [0 2 0]. From the SAED, the growth direction of SnO_2 nanowire was found to be [1 0 1], in agreement with previous reports [9,14]. The TEM observations showed that the growth behavior of the SnO_2 nanowires might not be dominated by the vapor–liquid–solid process proposed for a 1D nanostructure, in which a catalytic metal particle was located at the growth front and acts as the energetically favorable site [17]. Since no catalytic droplets observed on any end of the nanowires that was the most remarkable sign of the VLS mechanism. Therefore, we can reasonably speculate that the SnO_2 nanowires undergo a vapor–solid growth process.

Rutile SnO_2 belong to the point group D_{4h}^{14} and space group $P4_n/mnm$, of which the normal lattice vibration at the Γ point of the brillouin zone is given on basis of group theory:

$$\Gamma = A_{1g} + A_{2g} + B_{1g} + B_{2g} + E_g + 2A_{2u} + 2B_{1u} + 4E_u$$

Among them, the active Raman modes are B_{1g}, E_g, A_{1g}, and B_{2g}, and consequently four first-order Raman spectra are observed. In the Raman active modes the oxygen atoms vibrate while the Sn atoms are at rest. The modes of A_{1g} and B_{2g} vibrate in the plane perpendicular to the *c*-axis while the E_g mode vibrates in the direction of the *c*-axis [15].

The Raman peaks of the starting SnO_2 powder were detected at 474.7, 634.6, and 776.6 cm^{-1}, corresponding to the E_g, A_{1g}, and B_{2g} vibration modes of rutile bulk SnO_2, respectively. While the Raman peaks of the SnO_2 nanowires appeared at 475.0, 634.6, and 772.5 cm^{-1}. Thus, these peaks further confirm that SnO_2 nanowires possess the crystalline structure of the tetragonal rutile structure similar to that of the powder. In the Raman spectrum of the SnO_2 nanowires, the modes A_{1g} and B_{2g} shift toward lower wave numbers while the mode E_g shifts toward higher wave numbers. A small dimension of the nanowires leads to a downshift of the Raman peaks, while stress trends to shift Raman peak to a higher frequency region [15] (Fig. 4).

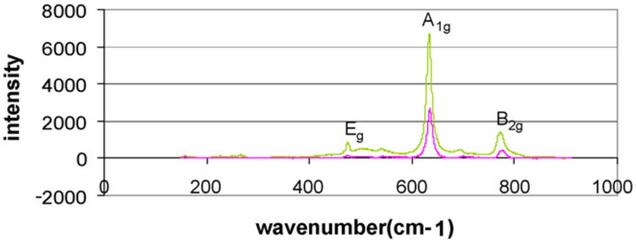

Fig. 4. Comparison of Raman spectrum which is a pink line from powder and a green line from nanowires. (For interpretation of the references to color in this figure legend, the reader is referred to the web version of the article.)

There are two models, at least, can be proposed to describe the growth mechanism of the one-dimensional materials, such as vapor–liquid–solid (VLS) and vapor–solid (VS) mechanisms. Presence of a tip growth is a key factor to verify the mechanism. The SEM in this work reveals that both mechanisms could be possible. In Fig. 2d a tip growth which represents VLS mechanism could be observed, although not much. Hence, it is likely that the growth of SnO_2 nanowires dominated by the vapor–solid (VS) mechanism [14].

In this report SnO_2 nanowires could be formed only when SnO, CuO and C were employed together. From this experience, our experimental results may be explained as follows. Firstly, CuO powder was reduced by active carbon powder at 700 °C yield Cu_2O and CO_2, described in the following reaction:

$$4CuO(s) + C(s) \xrightarrow{700\,^{\circ}C} 2Cu_2O(s) + CO_2(g) \quad (1)$$

Normally, the phase transformation from SnO to SnO_2 in an ambient atmosphere may be occurred as low as 370 °C [16] but usually in the powder form not the nanoform if heated alone. In this work, therefore, Cu_2O acted as a catalyst in the transformation of SnO to SnO_2 in the nanoform which could be explained by the chemical reaction between Cu_2O and SnO as following:

$$SnO(s) + Cu_2O(s) \xrightarrow{850\,^{\circ}C} SnO_2(s) + 2Cu(s) \quad (2)$$

Now, the nanoparticles of SnO_2 in (2) performed as nucleation sites and initiate the growth of SnO_2 nanowires via the VS mechanism [14,17].

To verify whether this chemical reaction brings out the nanoformation of SnO_2 wires, we simulated the reaction between Cu_2O and SnO directly in the ambient temperature at 850 °C and found that SnO_2 nanowires could be formed but the yield was low. The Cu from (2) can further react with O_2 to form CuO as the resultant:

$$2Cu_2O(s) + O_2(g) \rightarrow 4CuO(s) \tag{3}$$

Thus, this may be another possible factor whereas the decreasing of O_2 due to oxidation of CuO in reaction (3) which will lead to the formation of a smaller vapor of SnO_2 nuclei than the direct (higher pressure oxygen) oxidation of SnO at high temperature [18]. The smaller vapor of SnO_2 would likely be a dominant of smaller supersaturation to promote the growth of wire-like structure.

4. Conclusions

In summary, large-scale SnO_2 nanowires synthesized from SnO precursor under normal atmospheric pressure has been reported. The SnO_2 nanowires were about 100–800 μm in length with the width of 30–200 nm. These synthesized structures were single crystals and their growth direction was parallel to the [1 0 1] direction. The results from Raman spectra and XRD pattern indicated that these nanowires were rutile structure of SnO_2. The shift of the Raman spectrum to a lower frequency was associated with the size effect. VS mechanism of these nanostructures could open the new simple and low-cost fabrication technique on producing nanostructures of many materials. The large-scale SnO_2 nanowires reported here can be used as semiconductors, gas sensors and photocatalysts.

References

[1] A.P. Alivisatos, Semiconductor clusters, nanocrystals, and quantum dots, Science 271 (1996) 933–937.

[2] S. Frank, P. Poncharal, Z.L. Wang, W.A.D. Heer, Carbon nanotube quantum resistors, Science 280 (1998) 1744–1746.

[3] Z.Q. Jin, Y. Ding, Z.L. Wang, Mechanical behavior and magnetic separation of quasi-one-dimensional SnO_2 nanostructures: a technique for achieving monosize nanobelts/nanowires, J. Appl. Phys. 97 (2005), 74309 (1–5).

[4] S. Piscanec, A.C. Ferrari, M. Cantoro, S. Hofmann, J.A. Zapien, Y. Lifshitz, S.T. Lee, J. Robertson, Raman spectrum of silicon nanowires, Mater. Sci. Eng. C: Biosci. 23 (2003) 931–934.

[5] S.G. Anasari, P. Boroojerdian, S.R. Sainkar, R.N. Karekar, R.C. Aiyer, S.K. Kulkarni, Grain size effects on H_2 gas sensitivity of thick film resistor using SnO_2 nanoparticles, Thin Solid Films 295 (1997) 271–276.

[6] K.R. Prasad, N. Miura, Electrochemical synthesis and characterization of nanostructure tin oxide for electrochemical redox supercapacitors, Electrochem. Commun. 6 (2004) 849–852.

[7] G. Sberveglieri, Classical and novel techniques for the preparation of SnO_2 thin-film gas sensors, Sens. Actuator B: Chem. 6 (1992) 239–247.

[8] M. Turrion, J. Bisquert, P. Salvador, Flatband potential of F: SnO_2 in a TiO_2 dye-sensitized solar cell: an interference reflection study, J. Phys. Chem. B 107 (2003) 9397–94030.

[9] J.L. Gole, Z.L. Wang, SnO_x nanocrystallites supported by silica nanostructures, Nano Lett. 1 (2001) 449–451.

[10] Z.R. Dai, Z.W. Pan, Z.L. Wang, Growth and structure evolution of novel tin oxide nanodiskettes, J. Am. Chem. Soc. 124 (2002) 8673–8680.

[11] S.H. Sun, G.W. Meng, Y.W. Wang, T. Gao, M.G. Zhang, Y.T. Tian, X.S. Peng, L.D. Zhang, Large-scale synthesis of SnO_2 nanobelts, Appl. Phys. A 76 (2003) 287–289.

[12] C. Xu, X. Zhao, S. Liu, G. Wang, Large-scale synthesis of rutile SnO_2 nanorods, Solid State Commun. 125 (2003) 301–304.

[13] Z.L. Wang, Nanobelts, nanowires and nanodiskettes of semiconductor oxides—from materials to nanodevices, Adv. Mater. 15 (2003) 432–436.

[14] Z.R. Dai, Z.W. Pan, Z.L. Wang, Novel nanostructures of functional oxides synthesized by thermal evaporation, Adv. Funct. Mater. 13 (2003) 9–24.

[15] R.S. Katiyar, P. Dawson, M.M. Hargreave, G.R. Wilkinson, Dynamics of the rutile structure. III. Lattice dynamics, infrared and Raman spectra of SnO_2, J. Phys. C: Solid State Phys. 4 (1971) 2421–2431.

[16] D. Calestani, M. Zha, G. Salviati, L. Lazzarini, L. Zanotti, E. Comini, G. Sberveglieri, Nucleation and growth of SnO_2 nanowires, J. Cryst. Growth 275 (2005) e2083–e2087.

[17] S. Choopun, H. Tabata, T. Hawai, Self-assembly ZnO nanorods by pulsed laser deposition under argon atmosphere, J. Cryst. Growth 274 (2005) 167–172.

[18] J.K. Jian, X.L. Chen, W.J. Wang, L. Dai, Y.P. Xu, Growth and morphologies of large-scale SnO_2 nanowires, nanobelts and nanodendrites, Appl. Phys. A 76 (2003) 291–294.